Available online at www.sciencedirect.com

SciVerse ScienceDirect

Journal of the European Ceramic Society 32 (2012) 989–999

www.elsevier.com/locate/jeurceramsoc

Influence of thermal damage occurrence at microstructural scale on the thermomechanical behaviour of magnesia–spinel refractories

R. Grasset-Bourdel [a,c], A. Alzina [a,b], M. Huger [a], D. Gruber [c], H. Harmuth [c], T. Chotard [a,b,*]

[a] GEMH-ENSCI, CENTRE EUROPEEN de la CERAMIQUE, 12 rue Atlantis, 87065 Cedex Limoges, France
[b] IUT du Limousin, département GMP, 2 allée André Maurois, 87065 Limoges Cedex, France
[c] Chair of Ceramics, University of Leoben, Peter-Tunner-Straße 5, 8700 Leoben, Austria

Received 17 June 2011; received in revised form 25 October 2011; accepted 29 October 2011
Available online 14 December 2011

Abstract

Many refractory materials exhibit high thermal shock resistance, which is often mostly due to their high flexibility. Understanding the microstructure key points allowing to develop a non-linear mechanical behaviour is of great relevance for future material improvements. The present work aims at optimising the processing of magnesia–spinel refractory materials close to industrial ones with simplified microstructures. The final goal is the investigation of the relationship existing between microstructure evolutions and induced thermomechanical properties. The thermal expansion mismatch which exists between the two phases (spinel inclusions and magnesia matrix) is expected to generate, during cooling, radial microcracks around the inclusions. The development of such microcracks network, closely related to the inclusions content, has been studied and the damage occurrence has been confirmed by several high temperature characterisation techniques. The influence of this thermal micro damage on the evolution of stress–strain law in tension of such materials has also been investigated.

Keywords: Refractories; MgO; Spinels; Inclusions; Mechanical properties; Thermal shock resistance

1. Introduction

Due to their large panel of applications, refractory materials are used in many industrial areas such as the steel, cement, lime, non-ferrous metals and glass processing. Indeed, they can provide, first, high temperature resistance to specific parts required for many industrial installations. Moreover, if well selected, in accordance with the desired application, refractory materials can also ensure enhanced resistance against corrosion mechanisms and external mechanical loads. These features are essential to both increase the security of workers and save production costs. Nevertheless, in the special case of thermal shock applications, involving high local thermal stresses, the fulfilment of these previous required specifications is not sufficient to select the more appropriate refractory material. The thermal shock resistance of refractories is an old issue widely studied during the last decades[1–7] but still not fully explored, which is known to be closely related to their crack growth resistance and their "non-linear" mechanical behaviour (deviation from pure linear elasticity).[8–15] Because of many aspects, it is very difficult to predict the thermal and mechanical behaviour of refractory materials at a macroscopic scale. Nevertheless, it is well known that the difference of thermal expansion coefficients between phases induces a thermal expansion mismatch which is mainly responsible for the presence of microcracks and debonding in the microstructure of several refractories.[16–18] These "thermally damaged" materials often develop a non-linear stress–strain behaviour (growth of a diffuse microcracks network), a high fracture energy and, thus, take advantage of these characteristics for the enhancement of thermal shock resistance. This study is a part of a work aiming to understand the microstructure effects entailing non-linear mechanical behaviour by both experimental and numerical means. The two-phase refractory materials considered here are

* Corresponding author at: GEMH-ENSCI, CENTRE EUROPEEN de la CERAMIQUE, 12 rue Atlantis, 87065 Cedex Limoges, France.
Tel.: +33 5 87 50 25 60.
E-mail address: thierry.chotard@unilim.fr (T. Chotard).

0955-2219/$ – see front matter © 2011 Elsevier Ltd. All rights reserved.
doi:10.1016/j.jeurceramsoc.2011.10.048

magnesia–spinel materials with a thermal expansion mismatch between phases ($\Delta\alpha = \alpha_{inclusion} - \alpha_{matrix} < 0$) inducing radial microcracks within the magnesia matrix.

The first part of this study mainly consists in highlighting and quantifying the thermal damage in the different composites, which occurred during the cooling stage, by considering the Hashin and Shtrikman model as a reference. The second part focuses on the high temperature characterisation of the mechanisms responsible for this thermal damage. This characterisation will be carried out from room temperature to high temperature by a typical experimental tests package (high temperature ultrasonic characterisation, high temperature acoustic emission and thermal expansion measurements). Finally, the influence of this thermal damage on the non-linear mechanical behaviour of the material will be discussed in the third part.

2. Experimental

2.1. Materials

2.1.1. Single constituents

Concerning the raw materials used in this study, industrial magnesia (with low iron content) and sub-stoichiometric (MgO rich) spinel aggregates, from fines (<0.1 mm) up to aggregates of 1–3 mm (for spinel) or 3–5 mm (for magnesia), have been used for the processing of both single constituents samples and two-phase materials. The values of the bulk density and porosity of these magnesia and spinel aggregates (1–3 mm), as well as the true density of the magnesia and spinel powders (grain size <40 μm), are reported in the columns 2–4 of Table 1.

Concerning the processing routes, two different types of magnesia or spinel samples were fabricated, namely "disc samples" of small size with variable porosity and "bricks" of large size allowing to extract samples (by machining) for mechanical characterisation.

- The disc samples (diameter: 50 mm) were obtained by laboratory uniaxial pressing of fine powders of either magnesia or spinel. Porosity was here mainly introduced by changing the applied pressure, from 60 MPa to 7 MPa, but also by lowering the firing temperature (1300 °C instead of 1600 °C). The obtained porosity ranged between 17 and 32 vol.%, for magnesia samples, and between 8 and 19 vol.% for spinel samples (see Table 1). Since the idea was here to cover the potential porosity of the magnesia matrix within the composite materials, no forming agent has been considered. These samples were processed so as to get accurate relations between Young's modulus and porosity. Moreover, the knowledge of Young's modulus evolution versus porosity of magnesia also allows to estimate the actual Young's modulus of the magnesia matrix of each composite (if the density of samples differs from each others). Otherwise, these homogeneous materials are not thermally damaged since there is no anisotropic thermal expansion within the grains (cubic structures).
- The bricks were fabricated by semi-industrial production means, with a maximum pressure of 140 MPa and a maximum firing temperature of 1600 °C. The average dimensions are approximately 230 mm × 114 mm × 75 mm. Information concerning these bricks, such as density, porosity and thermal expansion coefficient, are given in Table 1. These bricks were processed in order to be able to carry out macro-scale experiments, like ultrasonic techniques and mechanical tests. Moreover, the magnesia brick was then, considered as a reference for the magnesia–spinel composites since their constitution were based on the same granulometry of magnesia grains.

2.1.2. Magnesia–spinel composites with different spinel inclusions contents

The magnesia–spinel composites, composed of a magnesia matrix and spinel inclusions, were processed according to the same pressure and heating cycles used for the magnesia and spinel bricks. The aim here was to produce composites consisting of a monophase matrix (magnesia) with introduced inclusions (spinel), which is easier to model numerically. For this reason, contrary to the usual definition of the term "matrix" which designates fines, in the present paper, the name "magnesia matrix" will represent the whole composite excepting the spinel inclusions (with coarse magnesia grains). This spinel content ranged between 5 wt.% and 34 wt.% for the main spinel grain size of 1–3 mm. A complementary composition of 15 wt.%, with the 0–1 mm grain size, was also processed. As previously mentioned, the grain size distributions of these two-phase materials were deduced from the composition of the magnesia reference brick. Indeed, the spinel aggregates content replaced the same content of magnesia aggregates having the same size (1–3 mm or 0–1 mm).

The properties of these magnesia–spinel materials are given in Table 2, with those of the pure magnesia brick for reference. It appears that, with increasing spinel content, the bulk density of the composites decreases and the open porosity increases. From the bulk densities of these composites and the bulk density of the spinel inclusions, assumed to be constant (3.41 g cm^{-3}), the bulk densities of the matrices, as well as their total porosities, have been calculated and reported in Table 2. Thus, the increase of spinel content induces an increase of the total porosity of the magnesia matrix. This can be due to the fact that densification, during sintering, is less well achieved when adding more and more inclusions in a homogeneous material (here magnesia). The presence of microcracks in such composites might also have an influence on these higher values of porosity.

An example of microstructure of these magnesia–spinel materials is shown in Fig. 1. As expected, the thermal expansion mismatch (Table 1) existing between the magnesia matrix ($\alpha = 13.3 \times 10^{-6}\,K^{-1}$) and the spinel inclusions ($\alpha = 8.9 \times 10^{-6}\,K^{-1}$) are responsible for the presence of radial microcracks around the spinel inclusions which appeared during the cooling stage of the process. For this reason, these composites are so-called thermally damaged materials.

2.2. Characterisation techniques

The study of the relation existing between the microstructure and the thermo-mechanical properties of the magnesia–spinel

Table 1
Properties of the magnesia and spinel used as matrix and inclusions, respectively, in magnesia–spinel composites.

Nature	Powder (<40 μm)	Aggregates (1–3 mm)		Porous disc samples	Bricks[a]		
	Absolute density ($g\,cm^{-3}$)	Bulk density ($g\,cm^{-3}$)	Close porosity (%)	Studied porosity range (%)	Bulk density ($g\,cm^{-3}$)	Total porosity (%)	Thermal expansion coefficient (200–400 °C) (K^{-1})
Magnesia	3.61	3.51	2.9	17–32	2.98	17.5	13.3×10^{-6}
Spinel	3.66	3.41	6.8	8–19	2.99	18.21	8.9×10^{-6}

[a] The magnesia brick is the reference brick for the composite materials.

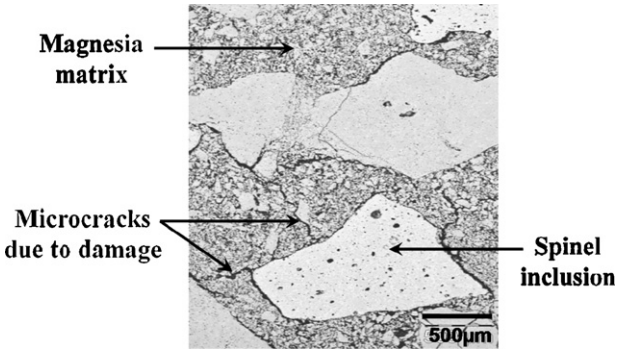

Fig. 1. Microstructure of a model magnesia–spinel composite.

composites needs to measure both the local and macroscopic properties of such materials. Therefore, at room temperature, the local Young's modulus of the aggregates was characterised by nano-indentation and ultrasonic means (in immersion), and the macroscopic Young's modulus of the samples was determined by a classical ultrasonic technique in contact. Then, thermal evolutions of macroscopic properties were studied by carrying out high temperature ultrasonic measurements, acoustic emission tests and thermal expansion measurements. The link between thermal damage during cooling and the macroscopic mechanical behaviour was finally investigated thanks to tensile tests.

2.2.1. Micro-scale techniques

The nano-indentation method allows to determine the local Young's modulus and hardness of the investigated grain. This technique consists in applying successive loading/unloading cycles on an indenter put in contact with the grain surface and to record the evolution of the applied load P versus depth h.[19,20] The experimental device[21] (Nanoindentation TM II) is composed of a diamond indenter in pyramid form with triangular base (Berkovich type[22]). The sample is first polished (∼1 μm) and, then, is stuck on a support monitored in displacement (0.1 μm). After determining the system rigidity S formed by the indenter/material couple and corresponding to the slope of the curve (dP/dh) during unloading, the local Young's modulus of the tested material is estimated. The volume of the measured zone, located under the indenter, is around several μm^3.

Complementary ultrasonic measurements in immersion (sample in water) were also realized on aggregates, confirming the results obtained by nano-indentation. The diameter of the tested aggregates is typically 2–3 mm with a thickness (parallel faces) of about 1–2 mm. This high frequency (80 MHz) ultrasonic technique, with no contact, provides the local Young's modulus of the considered aggregate from its density, its Poisson's ratio (assumed value) and the propagation velocity of the longitudinal wave within this aggregate.

2.2.2. Macro-scale techniques

The ultrasonic technique in contact (infinite mode) is a classical method (transducers in contact with the sample) to determine, at room temperature, the effective elastic properties, Young's modulus and Poisson's ratio, of a massive sample (here several centimetres). Measurements are performed in transmission at low frequency (1 MHz) so as to limit the waves attenuation due

Table 2
Properties of the magnesia/spinel composites and the magnesia reference brick.

	Magnesia reference brick	Magnesia–spinel composites								
		Spinel 1–3 mm								Spinel 0–1 mm
Spinel content	wt.%	0%	5%	10%	15%	20%	25%	30%	34%	15%
	vol.%	0%	4.3%	8.7%	13.0%	17.2%	21.5%	25.7%	29.2%	13.0%
Two-phase composite	Bulk density ($g\,cm^{-3}$)	2.98[a]	2.96	2.96	2.95	2.94	2.93	2.93	2.92	2.94
	Open porosity (%)	17.5%[a]	15.0%	15.1%	15.3%	15.4%	15.5%	15.6%	15.6%	15.8%
Magnesia matrix	Bulk density ($g\,cm^{-3}$)	2.98[a]	2.94[b]	2.91[b]	2.88[b]	2.84[b]	2.80[b]	2.76[b]	2.72[b]	2.87[b]
	Total porosity (%)	17.5%[a]	18.6%[b]	19.3%[b]	20.3%[b]	21.3%[b]	22.4%[b]	23.6%[b]	24.5%[b]	20.5%[b]

[a] These values of density/porosity correspond to those of the magnesia reference brick (without any spinel inclusion). Thus, values for the 0% inclusion – composite also correspond to those of the matrix.

[b] The properties of the matrices are here deduced from the properties of the composites taking into account spinel content and properties of spinel aggregates.

to the presence of inclusions or pores. The elastic properties are finally calculated from the wave velocities of both longitudinal and transversal propagation modes (two measurements) and the bulk density of the sample.[23,24]

Ultrasonic measurements at high temperature need to get the transducer away from the sample located in a furnace. Thus, the wave transmission is ensured through an alumina waveguide. The principle of this low frequency method in "long bar" mode (guided waves), based on the theory of Papadakis,[25] is detailed elsewhere.[26–28] Finally, this technique allows to calculate the Young's modulus E during the whole thermal cycle, from the bulk density ρ of the sample and the propagation velocity V_L of the longitudinal wave as follows:

$$E = \rho V_L^2 = \rho\left(\frac{2L}{\tau}\right)^2 \quad (1)$$

where L and τ are the length of the sample and the round trip time of the wave within the sample.

Typically, the sample dimensions were 150 mm × 11–14 mm × 11–14 mm, and the central frequencies of operating transducers were 40–80 kHz, depending on the considered composite. Measurements have been carried out during thermal cycles performed at a rate of 5 °C/min for heating and cooling stages with a 1 h isothermal dwell at 1350 °C.

Complementary thermal expansion measurements were carried out with a dilatometer (Setsys Evolution Setaram) with the same thermal cycle as high temperature ultrasonic measurements. Dimensions of the samples were approximately 20 mm × 8 mm × 8 mm.

Acoustic Emission experiments[29–31] were performed here in order to obtain complementary information about microstructure evolutions during thermal cycles, and especially on the chronology of *in situ* phenomena (damage mechanism occurrence), by analysing the evolution of the cumulated number of hits (recorded signals) versus temperature. The sample dimensions were the same for all the materials, namely 25 mm × 5.5 mm × 5.5 mm, and the same heating-cooling cycles as those quoted for ultrasonic and thermal expansion measurements were applied.

Tensile tests, providing the stress–strain laws of the studied material, were performed in order to investigate the relation between thermal damage, occurred during cooling, and the macroscopic mechanical behaviour. These tests were carried out with an INSTRON 8862 electromechanical device equipped with a specific alignment system.[32,33] Samples are constituted of a cylindrical rod (20 mm in diameter) with two metallic parts glued at each end. The final geometry is obtained by machining simultaneously the middle zone of the sample (diameter: 16 mm) and the metallic parts in order to get a perfect alignment with the loading axes. Tests performed at room temperature consist in applying a succession of loading/unloading cycles with a displacement increment at each beginning of cycle and with a constant displacement velocity (here around 1 $\mu m\,s^{-1}$). Strain variations are measured by two capacitive extensometers equipped with silicon carbide rods and placed on two opposite sides on the sample. The gauge length of each extensometer is 25 mm.

2.3. Analytical models used for thermo-elastic properties prediction

In addition to the experimental characterisation of thermo-mechanical properties of the two-phase materials (with either pores or inclusions), analytical models were used as references for the prediction of the evolution of the effective Young's modulus versus either pores (single constituents) or inclusions (magnesia–spinel composites) content in case of no thermal damage. Indeed, the Pabst–Gregorova model is used to provide the evolution of the Young's modulus of either magnesia or spinel versus porosity. The Hashin and Shtrikman model is used to get the hypothetical undamaged evolution of the Young's modulus of the magnesia–spinel composites versus inclusions content and, also, to quantify the thermal damage when the experimental values are lower than the analytical ones.

2.3.1. Pabst–Gregorova model as a reference for porous spinel and magnesia samples

The influence of porosity on the elastic properties is an old issue and many formulations have been proposed in the literature for several decades.[34–39] Pabst et al.[40] have reviewed some of these formulations and proposed a new one.[41] This model is expressed by:

$$E_r = \frac{E}{E_o} = (1 - [E]\phi + ([E] - 1)\phi^2)\left(\frac{1 - (\phi/\phi_c)}{1 - \phi}\right) \quad (2)$$

where E, E_0 and E_r are the Young modulus at the considered porosity, the dense Young modulus, and the relative Young modulus at the considered porosity; $[E]$ is a parameter to be determined by fitting experimentally measured data ($[E] = 2$ with isometric pores); ϕ, ϕ_c are the porosity and the percolation threshold, respectively.

This analytical model is used as reference for the study of the elastic properties of the single constituents versus porosity.

2.3.2. Hashin and Shtrikman model as a reference for undamaged magnesia–spinel materials

The model proposed by Hashin and Shtrikman[42–44] provides lower and upper bounds for the elastic properties (shear μ and bulk K moduli) of an isotropic two-phase material composed of a matrix and inclusions with perfect bonding at matrix/inclusion interfaces. The same kinds of bound were also proposed for the thermal expansion coefficient α.[45] Otherwise, lower and upper bounds of Young's modulus E can be deduced from the μ and K bounds for comparison with the experimental results. The HS^- lower bound is often cited in literature for its good description of the elastic behaviour of isotropic two-phase materials composed of stiff spherical inclusions within a softer matrix,[46] which is the case for the fabricated magnesia–spinel materials. Therefore, this lower bound will be used here as a reference value of E (and α) for an hypothetical undamaged magnesia–spinel material. Since, these composites are supposed to be thermally damaged, the comparison between experimental and reference analytical

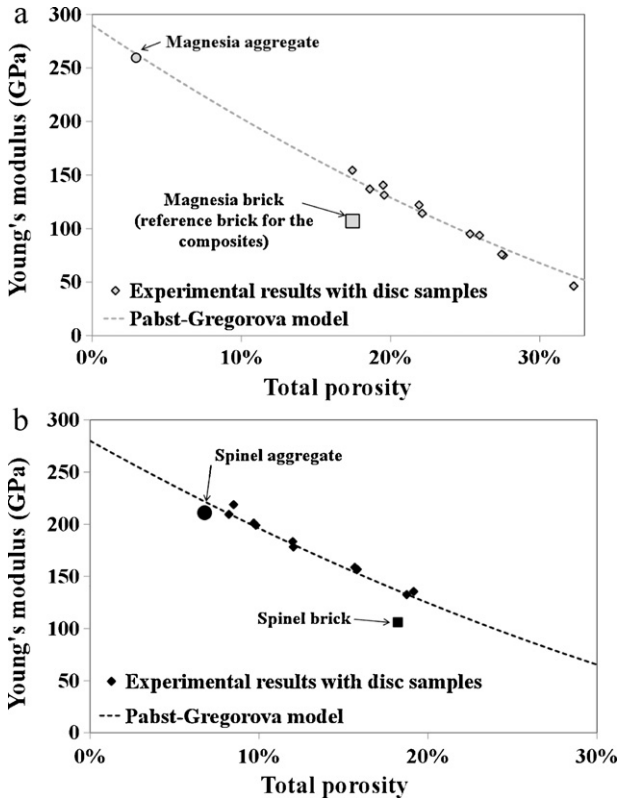

Fig. 2. Young's modulus evolution versus porosity of (a) magnesia (aggregate, disc samples and brick) and (b) spinel (aggregate, disc samples and brick), and comparison with the Pabst–Gregorova model.

values makes it possible to estimate the damage induced by CTE mismatch. The rather complex formulation of this model has been detailed in.[24]

3. Results and discussion

3.1. Elastic properties at room temperature

3.1.1. Single constituents: porosity influence

The experimental Young's modulus evolution versus porosity (different samples) of pure magnesia and pure spinel are shown in Fig. 2a and b, for a given porosity range. As expected, for both materials, the Young's modulus is significantly decreased by increasing the porosity. The analytical Pabst–Gregorova model is also represented in Fig. 2a and b. The value of the geometrical parameter [E] was fixed to 2 for both magnesia and spinel by assuming the pores to be isometric. These analytical values were obtained, by fitting the experimental results, for a percolation threshold ϕ_c assumed to be equal to 45% and values of dense Young's modulus E_0 of magnesia and spinel assumed to be equal to 290 and 280 GPa, respectively. As a remark, the value of E_0 for magnesia, deduced here, is slightly lower than the value obtained by Chung[47] on magnesia monocrystals and polycrystals, namely 305 GPa, from the stiffness constants C_{ij}. According to Fig. 2a and b, the Pabst–Gregorova seems to describe well the Young's modulus evolution versus porosity of both magnesia and spinel. Indeed, the values obtained on single aggregates

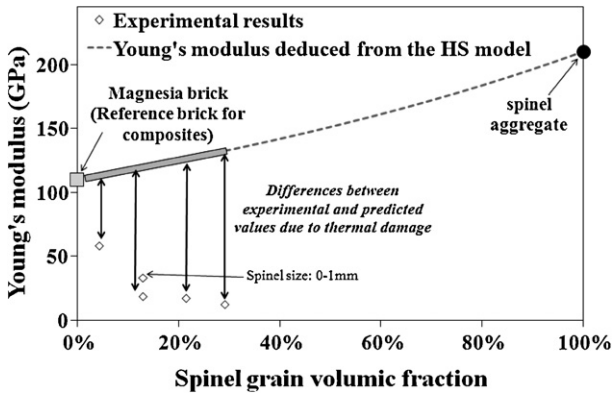

Fig. 3. Evolution of experimental Young's modulus of the magnesia–spinel composites versus spinel inclusions content and comparison with the lower bound of the Hashin and Strikman model.

by both nano-indentation (and local ultrasonic measurements in immersion) are very close to this model, as well as the values obtained on disc samples by ultrasonic means. Nevertheless, the experimental values obtained on bricks are quite lower than the analytical values. Since the disc samples are obtained only from fines and the bricks from different granulometric categories (fines, 0–1 mm and 1–3 mm grains), these lower results could come from the more complex microstructures of bricks with, for example, imperfect bond between aggregates and fines.

Finally, the experimental results obtained on spinel aggregates and on the magnesia reference brick are considered, in the next paragraph, as the values of Young's modulus of the two constituents of the magnesia–spinel composites, namely the spinel aggregates and the magnesia matrix.

3.1.2. Magnesia–spinel composites: spinel content influence and comparison with the Hashin and Shtrikman model

The experimental Young's modulus values previously obtained for the magnesia matrix and the spinel inclusions, namely 110 GPa and 210 GPa respectively, are considered in Fig. 3 representing the Young's modulus evolution versus spinel inclusions content of the magnesia–spinel composites. These two values, corresponding, respectively, to 0% and 100% of spinel inclusions allow to deduce the lower bound of the Hashin and Shtrikman model (Fig. 3) representing the hypothetical undamaged evolution of Young's modulus versus inclusions content. As a remark, due to their high heterogeneities, the experimental Young's modulus of the magnesia–spinel composites (bricks) were not obtained by usual ultrasonic measurements in infinite medium mode but by ultrasonic measurements in long bar mode allowing to work at lower frequencies.

As we could expect, the experimental and analytical results are not well correlated. According to the HS model, an increasing spinel inclusion content should increase Young's modulus of the composite, which is not observed experimentally. Indeed, it appears that increasing the spinel inclusion fraction induces a fall in Young's modulus.

In fact, lower Young's modulus values are in agreement with the presence of a microcracks network in these thermally

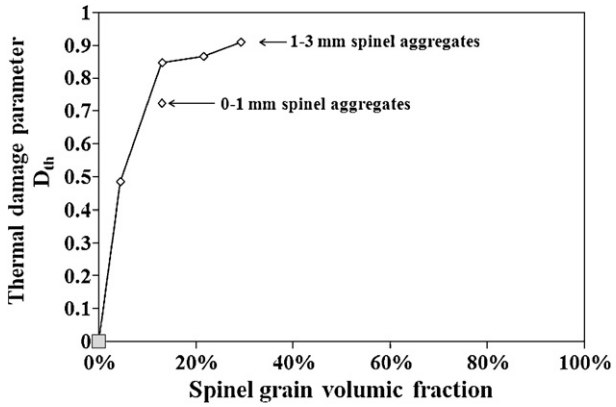

Fig. 4. Evolution of the *D*th thermal damage parameter, calculated from the experimental and theoretical (HS model) Young's modulus values.

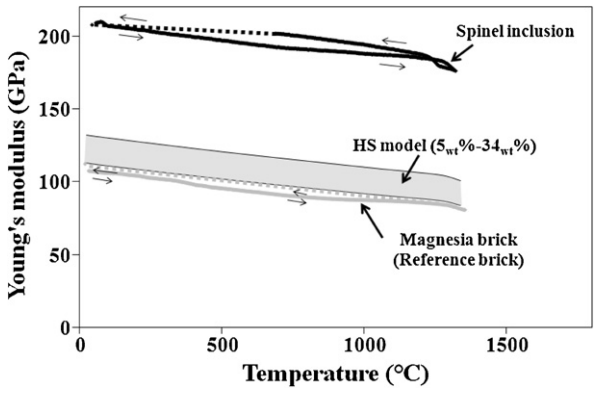

Fig. 5. Young's modulus evolutions versus temperature of the two single constituents and theoretical evolutions (HS model) of the magnesia–spinel composites.

damaged materials. Then, the spinel inclusion content (with a grain size of 1–3 mm) seems to have a very high impact on the results since only 5 wt.% is enough to divide the Young's modulus by two. Furthermore, the composite containing 15 wt.% of 0–1 mm spinel grains exhibits a higher Young's modulus than the one composed of 15 wt.% of 1–3 mm spinel grains. Thus, the elastic properties at room temperature seem to be less affected with smaller inclusions. As a remark, Aksel and Riley[48] studied the influence of the addition of spinel inclusions within a magnesia matrix, but for fine-grained magnesia–spinel composites (several tens of micrometers), involving much higher Young's modulus values, and observed also a decrease of Young's modulus versus spinel content.

As mentioned before, thermal damage can be estimated by calculating the gap (%) to the Hashin and Shtrikman lower bound:

$$D\text{th} = \frac{(E_{\text{HS}^-} - E_{\text{exp}})}{E_{\text{HS}^-}} \quad (3)$$

where *D*th, $E_{\text{HS}}-$ and E_{exp} are a "Kachanov"[49] thermal damage parameter, the analytical (HS model) and the experimental Young's modulus values, respectively.

Fig. 4 shows that the relation between the spinel content and the thermal damage parameter is not linear. In order to clarify the influence of the spinel inclusions (content and size) on the thermal damage of composites, high temperature investigations have been carried out and are presented in the next paragraph.

3.2. High temperature evolutions: thermal micro damage during cooling

3.2.1. Young's modulus evolution versus temperature

In first step, the Young's modulus evolutions versus temperature of the two single constituents of the composites were determined. To do that, long bar samples were extracted from processed bricks. For magnesia matrix, the magnesia reference brick, previously presented, is considered. For spinel inclusions, since it is not possible to characterise their Young's modulus at high temperature, a spinel brick has been processed (as shown in Fig. 2b). Then, since the porosity of this spinel brick is much higher, and the Young's modulus much lower, than the one of a spinel aggregate (Fig. 2b), the Young's modulus evolution versus temperature of a spinel aggregate has been recalculated, as finally presented in Fig. 5.

According to this figure, Young's modulus evolutions of the magnesia matrix and the spinel inclusions versus temperature are quasi-linear, reversible and exhibit almost the same slope. Moreover, from these two evolutions, a theoretical undamaged evolution zone, provided by the Hashin and Shtrikman model for the magnesia–spinel composites and corresponding to a spinel content between 5 and 34 wt.% have been added in Fig. 5.

In a second step, the Young's modulus evolutions versus temperature of the magnesia–spinel composites were determined and compared to the Hashin and Shtrikman model. These experimental evolutions are shown in Fig. 6a, with a spinel grain size of 1–3 mm and different spinel contents (5–34 wt.%), and in Fig. 6b, with a spinel content of 15 wt.% and different spinel grain sizes (0–1 mm and 1–3 mm). First, as already observed in Fig. 3, the experimental values at room temperature are far below the analytical ones. Then, by considering the whole curves, it appears that the combination of the two single constituents provides hysteretic Young's modulus evolutions with a value at room temperature much lower than those of magnesia or spinel alone. This is characteristic of thermally damaged materials with microcracks in the microstructure[18]: the high increase and decrease of Young's modulus during thermal cycle are mainly due to microcracks closure (heating) and microcracks opening (cooling), respectively. The temperature corresponding to the beginning of crack opening, characterised by the maximum value, during cooling, seems to be the same for all of the model materials, namely 950 °C approximately. Then, the major decrease in Young's modulus occurs in the 950–600 °C range, approximately. According to the results obtained with 1–3 mm spinel inclusions (Fig. 6a), a higher spinel content induces a lower Young's modulus value at room temperature (already discussed in Fig. 3). Of course, when temperature increases, the effect of thermal expansion mismatch tends to close microcracks and Young's modulus increases for all the composite materials, but the same classification is still observed at high temperature. In case of a fully crack healing, Young's modulus of composites should reach the estimated values of an hypothetical

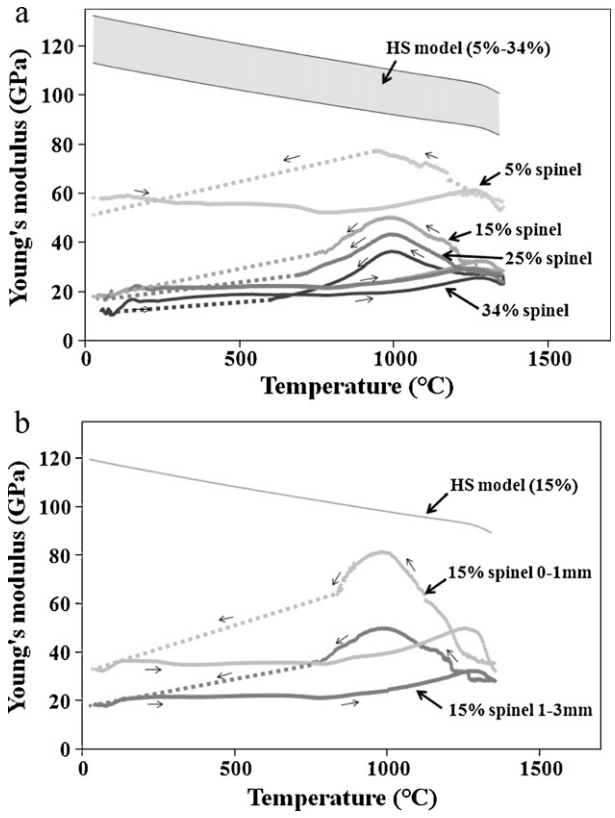

Fig. 6. Young's modulus evolutions versus temperature of the magnesia–spinel composites with a spinel grain size of 1–3 mm and different spinel contents (a) and with a spinel content of 15 wt.% and different spinel grain sizes (b).

non-microcracked material (HS model). In fact, the maximum value at 950 °C during cooling being rather lower than these values, it seems that, even at high temperature, microcracks are not fully closed within the different composite materials.

According to Fig. 6b, the 0–1 mm composite exhibits a Young's modulus at room temperature higher than the 1–3 mm composite (as already shown in Fig. 3). Moreover, the relative amplitude of the increase/decrease of Young's modulus appears to be much higher for the 0–1 mm composite than for the 1–3 mm composite. In other words, smaller spinel inclusions involve higher Young's modulus values at room temperature (lower damage within the microstructure), and higher increase in Young's modulus during heating (easier microcracks closure). A possible explanation could be that microcracks, present in the microstructure of the 0–1 mm composite, are smaller but more numerous. Indeed, this would justify the fact that the Young's modulus values are higher at room temperature. In addition, smaller microcracks could also facilitate closure mechanisms at high temperature.

As an additional remark, the measurement of Young's modulus during the final stage of cooling is usually not possible due to the breaking of the alumina cement, used to stick the sample to the waveguide, because of thermal expansion mismatch between this alumina cement and the magnesia–spinel sample. By re-measuring the Young's modulus at room temperature after the thermal cycle, the final evolution at the ending period of cooling is assumed and plotted in dotted line (Fig. 6a). The fact

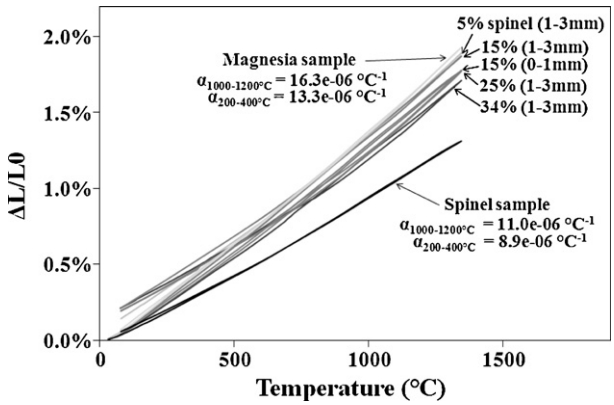

Fig. 7. Thermal expansion evolutions of the magnesia/spinel composites and the two constituents.

that the thermal expansion mismatch is higher when the spinel content is lower justifies the fact that the loss of signal appears earlier during cooling with the pure magnesia sample and the 5% composite.

3.2.2. Thermal expansion evolution

Thermal expansion evolutions of both single constituents and magnesia/spinel materials are presented in Fig. 7. Firstly, the significant difference between the curves slopes of the magnesia and spinel samples highlights the thermal expansion mismatch existing between the two phases of the magnesia–spinel composites. Moreover, these two thermal expansion curves are not linear (slopes at low and high temperature being quite different) but reversible. Concerning the two-phase materials, the overall shape of the curves is closely related to the spinel inclusion volume fraction. During cooling, the slopes decrease significantly, especially at the end of cooling, which entails rather small residual thermal strain (irreversible curves).

Furthermore, it has been observed previously that microcracks opening occurs during cooling, below 1000 °C. Therefore, it may be of interest to determine the thermal expansion coefficients of the magnesia–spinel composites during cooling, above and below this temperature and to compare these values with the Hashin and Shtrikman model. A high difference between experimental and analytical results could again confirm microcracking. Thus, the evolution of the thermal expansion coefficient versus the spinel inclusion content at both the beginning (1200–1000 °C) and the end of cooling (400–200 °C) are shown in Fig. 8. It appears that the thermal expansion coefficients measured at the beginning of cooling are in very good agreement with the lower bound of the Hashin and Shtrikman model whereas those measured at the end of cooling are not so close to these analytical values. Indeed, these measured values are lower than this model and the relative difference seems to increase slightly when the spinel content increases. According to these observations, a huge part of the microcracks present in the microstructure seems to be closed at the beginning of cooling. At lower temperature, stress relaxation, involved by microcracks opening during cooling, leads to lower thermal expansion values than expected.

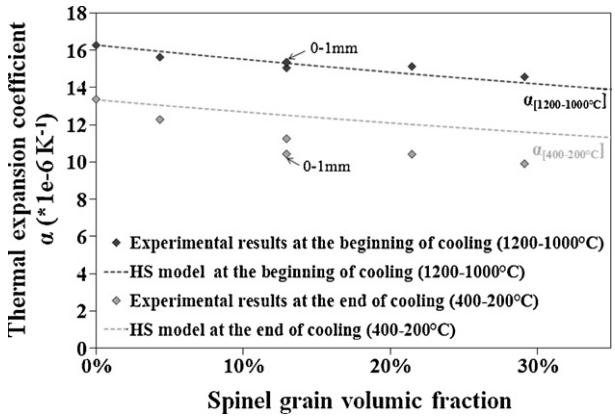

Fig. 8. Influence of the spinel inclusion content on the thermal expansion coefficient of composites at both the beginning (1200–1000 °C) and the end (400–200 °C) of cooling.

3.2.3. High temperature acoustic emission evolution

Acoustic emission tests at high temperature were also carried out in order to validate the hypothesis of microcracks opening during cooling, below 1000 °C, and to compare the results for the different magnesia–spinel composites. The acoustic emission results obtained for some of the considered materials are shown in Fig. 9a and b. According to Fig. 9a, the acoustic activity of a magnesia sample is very low (close to zero) compared to those of the other materials. For these two model materials (5 wt.% and 15 wt.% of spinel), acoustic activity is slightly present during heating, but is much higher during cooling, especially between 950 °C and 550 °C. This is in good agreement with the previous observations regarding Young's modulus evolutions versus temperature. Indeed, the presence of a quite small number of hits during heating can be explained by the mechanical closure of microcracks[29] whereas the sudden high increase of hits during the cooling stage may be interpreted as the re-opening of microcracks caused by thermal expansion mismatches. Moreover, Fig. 9a shows that a higher spinel content in model materials induces a higher cumulated number of hits during thermal cycling. This can be explained by the fact that more microcracks get opened during cooling when the spinel content is higher, as already proposed from Fig. 6a.

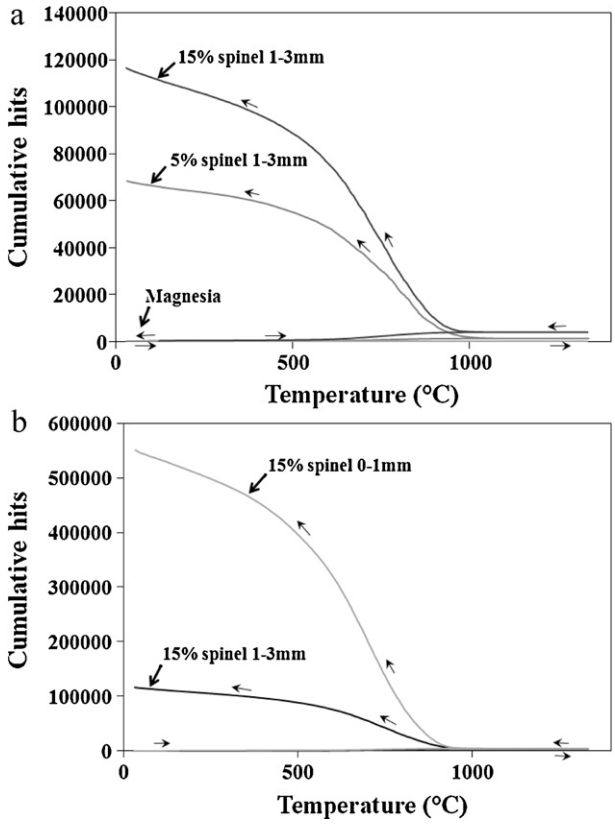

Fig. 9. Evolution of acoustic emission versus temperature during thermal cycle up to 1350 °C – influence of the spinel inclusions content (a) and the spinel grain size (b).

Furthermore, according to Fig. 9b, a smaller inclusion size seems to increase significantly the total cumulated number of hits. This would justify the fact that, as previously assumed from Fig. 6b, the number of microcracks in the 0–1 mm composite is higher than the one in the 1–3 mm composite, even if these "small" microcracks affect less the Young's modulus value.

3.3. Influence of thermal micro damage on the non-linearity of the stress–strain law in tension

As already mentioned in the introduction, the non-linearity of the mechanical behaviour allows to improve the thermal shock resistance. Then, it seemed interesting to investigate the influence of the spinel inclusions content, and, so, the thermal damage resulting from the cooling stage of the process, on the non-linearity of the stress–strain law in tension. Therefore, all the magnesia–spinel composites, as well as the single constituents, were characterised in tension. But, in order to be able to compare clearly the global curves, only three of them are represented in Fig. 10a, namely 5, 15 and 25% of spinel inclusions (1–3 mm). According to this figure, the global stress–strain curves in tension present a non-linear mechanical behaviour up to the peak with a significant post-peak region and residual strain when unloading. Moreover, the increase of spinel content seems mainly to decrease the tensile strength. The early beginning of the stress–strain curves of the different composites, as well as the single constituents are presented in Fig. 10b. As it could be expected, an increasing spinel inclusions content increases the non-linearity of the mechanical behaviour in tension due to a denser pre-existent microcracks network developed during cooling. The evolution of the tensile strength of the composites versus the thermal damage parameter Dth is represented in Fig. 11a. The increase of thermal damage obviously decreases the tensile strength, and the relation between the tensile strength and the thermal damage parameter appears quasi-linear, which means that these two results are very well correlated.

From the envelopes of the different global stress–strain curves of the composites, the fracture energies (in $J\,m^{-2}$) were calculated by considering the section of the sample. Then, the evolution of the fracture energy versus Dth is reported in Fig. 11b. First, it can be pointed out that the fracture energy

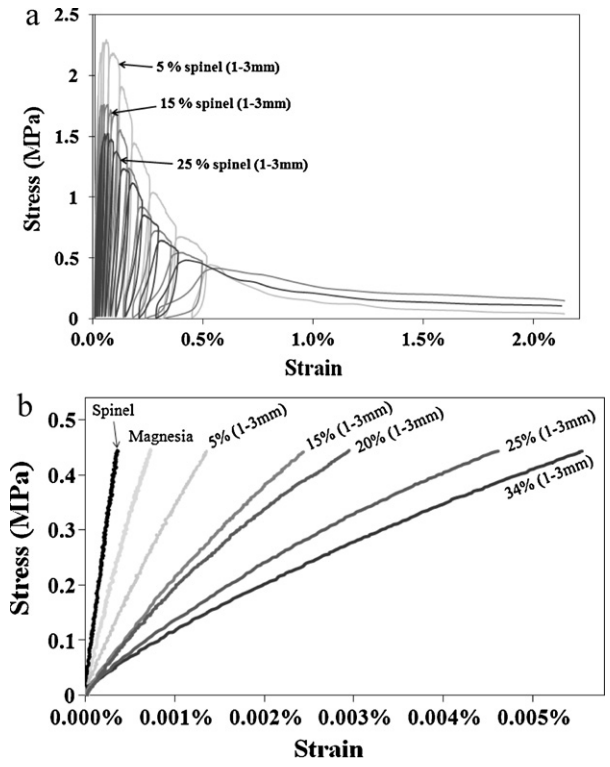

Fig. 10. (a) Global stress–strain curves of three different magnesia–spinel composites (5, 15 and 25 wt.% of spinel); (b) beginning of the stress–strain curves of the magnesia–spinel composites and the single constituents.

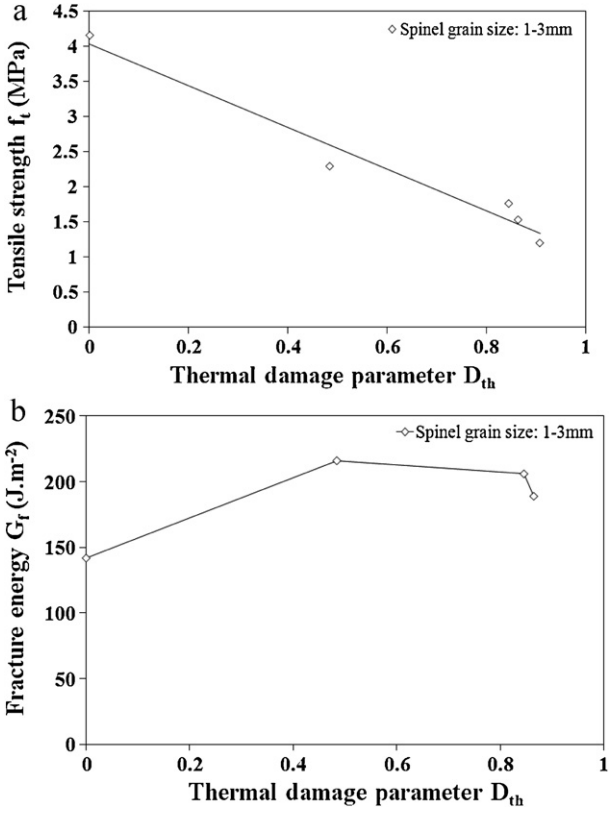

Fig. 11. Evolution of the tensile strength (a) and the fracture energy (b) of the composites versus the thermal damage parameter.

of the pure magnesia material, without any addition of spinel inclusions, is already significant compared to common ceramics. Indeed, magnesia is known to be not brittle but "quasi-brittle" which may explain this rather high value. Secondly, it appears that the addition of spinel allows to increase the fracture energy. Indeed, with only 5 wt.% of spinel inclusions, the thermal damage is rather high (around 0.5) and the increase in fracture energy is about 50%. Nevertheless, with higher spinel contents, and, so, higher thermal damage, the fracture energy is no longer increased but remains in the same range. This increase of fracture energy is in the same range as the one (work-of-fracture) observed by Aksel and Riley[48] with fine-grained composites. Furthermore, Harmuth et al.[50,51] showed that an industrial magnesia–spinel product does not necessarily present a higher specific fracture energy than an industrial pure magnesia product due to its much lower tensile strength. Thus, they proposed to quantify the ratio of fracture energy to tensile strength, which might be considered as an indicator of brittleness.

4. Conclusion

This study aimed at a better understanding of the thermo-mechanical behaviour of refractories in relation with their microstructures. To achieve that, magnesia–spinel composites were processed. The thermal expansion mismatch between the two phases entails radial matrix microcracking around the spinel inclusions. The Hashin and Shtrikman model was applied, here, as a reference to quantify the thermal damage present in those two-phase materials. Indeed, by calculation of a thermal damage parameter, the influence of the spinel content on thermal damage could be estimated. Moreover, the comparison of the Young's modulus at high temperature (beginning of cooling) with the values predicted by this model allowed to show that microcracks present in these materials are not fully closed at the maximum temperature of the thermal cycle. As expected, the studied magnesia/spinel composites exhibit non-linear mechanical behaviour in tension up to the peak, significant post-peak evolutions, high strain-to-rupture values and residual strain when unloading. The considered spinel content range allowed to modulate the damage rate, present as a diffuse microcracks network, in order to analyse the influence of this thermal damage on the mechanical damage growth within the composites (non-linearity) when loaded. Thus, it was observed that the increase of the spinel content has a real influence on the non-linearity of the mechanical behaviour and that the increase of the thermal damage highly decreases the tensile strength and increases the fracture energy. Such increase of fracture energy, linked to an increase of strain to rupture, is of particulate interest for thermal shock applications.

Acknowledgements

Financial support by the Austrian Federal Government and the Styrian Provincial Government (Österreichische Forschungs förderungsgesellschaft and Steirische Wirtschafts förderungs-gesellschaft) within the K2 Competence Centre on "Integrated

Research in Materials, Processing and Product Engineering" (MCL Leoben) in the framework of the Austrian COMET Competence Centre Programme, is gratefully acknowledged.

References

1. Kingery WD. Factors affecting thermal stress resistance of ceramics materials. *J Am Ceram Soc* 1955;**38**(1):3–15.
2. Hasselman DPH. Elastic energy at fracture and surface energy as design criteria for thermal shock. *J Am Ceram Soc* 1963;**46**(11):535–40.
3. Hasselman DPH. Unified theory of thermal shock fracture initiation and crack propagation in brittle ceramics. *J Am Ceram Soc* 1969;**52**(11): 600–4.
4. Nakayama J. Direct measurement of fracture energies of brittle heterogeneous materials. *J Am Ceram Soc* 1965;**48**(11):583–7.
5. Aksel C, Rand B, Riley FL, Warren PD. Thermal shock behaviour of magnesia–spinel composites. *J Eur Ceram Soc* 2004;**24**(9):2839–45.
6. Boccaccini DN, Cannio M, Volkov-Husoviæ TD, Kamseu E, Romagnoli M, Veronesi P, et al. Service life prediction for refractory materials. *J Mater Sci* 2008;**43**:4079–90.
7. Schmitt N, Burr A, Berthaud Y, Poirier J. Micromechanics applied to the thermal shock behaviour of refractory ceramics. *Mech Mater* 2002;**34**(11):725–47.
8. Steinbrech RW, Knehans R, Schaarwaechter W. Increase of crack resistance during slow crack growth in Al_2O_3 bend specimens. *J Mater Sci* 1983;**18**:265–70.
9. Sakai M, Bradt RC. Fracture toughness testing of brittle materials. *Int Mater Rev* 1993;**38**(2):53–78.
10. Adams A, Landini DJ, Schmacher CA, Bradt RC. Micro- and macrocrack growth in alumina refractories. *Bull Amer Cer Soc* 1981;**60**(7): 730–5.
11. Harmuth H, Rieder K, Krobath M, Tschegg EK. Investigation of the nonlinear fracture behaviour of ordinary ceramic refractory materials. *Mater Sci Eng A* 1996;**214**(1–2):53–61.
12. Simonin F, Olagnon C, Maximilien S, Fantozzi G, Diaz LA, Torrecillas R. Thermo-mechanical behaviour of high-alumina refractory castables with synthetic spinel additions. *J Am Ceram Soc* 2000;**83**:2481–90.
13. Huebner H, Jillek W. Sub-critical crack extension and crack resistance in polycrystalline alumina. *J Mater Sci* 1977;**12**:117–25.
14. Sakai M, Bradt RC. Graphical methods for determining the nonlinear fracture parameters of silica and carbon refractory composites. In: Bradt RC, editor. *Fracture mechanics of ceramics*, vol. VII. New York, NY: Plenum Publishing Corp.; 1986. p. 127–42.
15. Lutz HE, Claussen N, Swain MV. KR-curve behavior of duplex ceramics. *J Am Ceram Soc* 1991;**74**(1):11–8.
16. Soady JS, Plint S. A quantitative thermal shock approach to the development of magnesia–spinel refractories for the cement kiln. In: *UNITECR 91*. 1991. p. 443–9.
17. Aksel C, Rand B, Riley FL, Warren PD. Mechanical properties of magnesia–spinel composites. *J Eur Ceram Soc* 2002;**22**(5):745–54.
18. Huger M, Tessier-Doyen N, Chotard T, Gault C. Microstructural effects associated to CTE mismatch for enhancing the thermal shock resistance of refractories: investigation by high temperature ultrasounds. *Ceram Forum Int fi/Ber DKG* 2007;**84**(9):93–103.
19. Lagrange JL, Passilly B, Parlier M, Colomban P.*Détermination des Propriétés Mécaniques Locales des Constituants de Composites Céramique-Céramique*. 1992.
20. Paletto S, Fantozzi G. Nanoindentation: théorie et applications. *Rev Comp Mater Avancés* 1993;**3**(2):139–60.
21. Deniel S, Tessier-Doyen N, Dublanche-Tixier C, Chateigner D, Blanchart P. Processing and characterization of textured mullite ceramics from phyllosilicates. *J Eur Ceram Soc* 2010;**30**(12):2427–34.
22. Oliver WC, Pharr MG. An improved technique for determining hardness and elastic modulus using load and displacement sensing indentation experiments. *J Mater Res* 1992;**7**(6):1564–83.
23. Mason WP. *Physical acoustics*, vol. 1., part A. London: Academic Press; 1964. p. 174.
24. Grasset-Bourdel R, Alzina A, Tessier-Doyen N, Huger M, Chotard T, Schmitt N, et al. Optimization of 3D RVE for anisotropy index reduction in modelling thermoelastic properties of two-phase composites using a periodic homogenisation method. *Comput Mater Sci* 2011;**50**: 3136–44.
25. Papadakis EP. Ultrasonic measurements of Young's modulus and extensional wave attenuation in refractory: metal wires at elevated temperature with application to ultrasonic thermometry. *J Appl Phys* 1974;**45**(6): 2409–20.
26. Gault C, Platon F, Le Bras D. Ultrasonic measurement of Young modulus of Al2O3-based refractories at high temperatures. *Mater Sci Eng* 1985;**74**:101–11.
27. Cutard T, Fargeot D, Gault C, Huger M. Time delay and phase shift measurement for ultrasonic pulses using auto correlation methods. *J Appl Phys* 1994;**75**(4):1909–13.
28. Huger M, Fargeot D, Gault C. High-temperature measurement of ultrasonic wave velocity in refractory materials. *High Temp High Press* 2002;**34**:193–201.
29. Chotard T, Soro J, Lemercier H, Huger M, Gault C. High temperature characterization of Cordierite–Mullite refractory by ultrasonic means. *J Eur Ceram Soc* 2008;**28**:2129–35.
30. Briche G, Tessier-Doyen N, Huger M, Chotard T. Investigation of damage behaviour of refractory model materials at high temperature by combined pulse echography and acoustic emission techniques. *J Eur Ceram Soc* 2008;**28**:2835–43.
31. Patapy C, Proust A, Marlot D, Huger M, Chotard T. Characterization by acoustic emission pattern recognition of microstructure evolution in a fused-cast refractory during high temperature cycling. *J Eur Ceram Soc* 2010;**30**(15):3093–101.
32. Ghassemi Kakroudi M, Yeugo-Fogaing E, Gault C, Huger M, Chotard T. Effect of thermal treatment on damage mechanical behaviour of refractory castables: comparison between bauxite and andalusite aggregates. *J Eur Ceram Soc* 2008;**28**:2471–8.
33. Ghassemi Kakroudi M, Huger M, Gault C, Chotard T. Damage evaluation of two alumina refractory castables. *J Eur Ceram Soc* 2009;**29**:2211–8.
34. Spriggs RM. Expression for effect of porosity on elastic modulus of polycrystalline refractory materials, particularly aluminum oxide. *J Am Ceram Soc* 1961;**44**:628–9.
35. Ishai O, Cohen LJ. Elastic properties of filled and porous epoxy composites. *Int J Mech Sci* 1967;**9**(8):539–46.
36. Coble RL, Kingery WD. Effect of porosity on physical properties of sintered alumina. *J Am Ceram Soc* 1956;**39**:377–85.
37. Mackenzie JK. The elastic constants of a solid containing spherical holes. *Proc Phys Soc Lond B* 1950;**63**:2–11.
38. Nemat-Nasser S, Hori M. *Micromechanics-overall properties of heterogeneous materials*. 2nd ed. Amsterdam: North-Holland/Elsevier; 1999. pp. 1–786.
39. Christensen RM. Mechanics of cellular and other low-density materials. *Int J Solids Struct* 2000;**37**:93–104.
40. Pabst W, Gregorova E, Ticha G. Elasticity of porous ceramics – a critical study of modulus – porosity relations. *J Eur Ceram Soc* 2006;**26**:1085–97.
41. Pabst W, Gregorova E. New relation for the porosity dependence of the effective tensile modulus of brittle materials. *J Mater Sci* 2004;**39**: 3501–3.
42. Hashin Z. The elastic moduli of heterogeneous materials. *J Appl Mech* 1962;**29**(1):143–50.
43. Hashin Z, Shtrikman S. On some variational principles in anisotropic and nonhomogeneous elasticity. *J Mech Phys Solids* 1962;**10**:335–42.
44. Hashin Z, Shtrikman S. A variational approach to the theory of the elastic behavior of multiphase materials. *J Mech Phys Solids* 1963;**11**: 127–40.
45. Rosen BW, Hashin Z. Effective thermal expansion coefficients and specific heats of composite materials. *Int J Eng Sci* 1970;**8**:157–73.
46. Tessier-Doyen N, Glandus JC, Huger M. Experimental and numerical study of elastic behavior of heterogeneous model materials with spherical inclusions. *J Mater Sci* 2007;**42**:5826–34.
47. Chung DH. Elastic moduli of single crystal and polycrystalline MgO. *Philos Mag* 1963;**8**(89):833–41.

48. Aksel C, Riley FL. Effect of the particle size distribution of spinel on the mechanical properties and thermal shock performance of MgO–spinel composites. *J Eur Ceram Soc* 2003;**23**(16):3079–87.
49. Kachanov LM. Time of the rupture process under creep conditions. *Izv Akad Nauk SSR Otd Tech Nauk* 1958;**8**:26–31.
50. Harmuth H. Characterisation of the fracture path in 'flexible' refractories. In: *12th International Ceramics Congress CIMTEC 2010*. 2010.
51. Harmuth H, Bradt RC. Investigation of refractory brittleness by fracture mechanical and fractographic methods. In: *Refractories Manual 2010.*; 2010.